ADVANCES IN ATMOSPHERIC SCIENCES, VOL. 30, NO. 4, 2013, 1106–1116

Interaction between Adjacent Lightning Discharges in Clouds

WANG Yanhui*(王彦辉), ZHANG Guangshu (张广庶), ZHANG Tong (张 彤), LI Yajun (李亚珺), WU Bin (武 斌), and ZHANG Tinglong (张廷龙)

Laboratory of Land Surface Process and Climate Change in Cold and Arid Regions,

Cold and Arid Regions Environmental and Engineering Research Institute,

Chinese Academy of Sciences, Lanzhou, Gansu 730000

(Received 10 February 2012; revised 25 October 2012; accepted 2 November 2012)

ABSTRACT

Using a 3D lightning radiation source locating system (LLS), three pairs of associated lightning discharges (two or more adjacent lightning discharges following an arbitrary rule that their space-gap was less than 10 km and their time-gap was less than 800 ms) were observed, and the interaction between associated lightning discharges was analyzed. All these three pairs of associated lightning discharges were found to involve three or more charge regions (the ground was considered as a special charge region). Moreover, at least one charge region involved two lightning discharges per pair of associated lightning discharges. Identified from electric field changes, the subsequent lightning discharges were suppressed by the prior lightning discharges. However, it is possible that the prior lightning discharge provided a remaining discharge channel to facilitate the subsequent lightning discharge. The third case provided evidence of this possibility. Together, the results suggested that, if the charges in the main negative charge region can be consumed using artificial lightning above the main negative charge regions, lightning accidents on the ground could be greatly reduced, on the condition that the height of the main negative charge region and the charge intensity of the lower positive charge region are suitable.

Key words: associated lightning, inverted-polarity intracloud discharge, charge region, electrical structure

Citation: Wang, Y. H., G. S. Zhang, T. Zhang, Y. J. Li, B. Wu, and T. L. Zhang, 2013: Interaction between adjacent lightning discharges in clouds. *Adv. Atmos. Sci.*, **30**(4), 1106–1116, doi: 10.1007/s00376-012-2008-9.

1. Introduction

Mazur (1982) suggested that there can be an association between closely spaced, sequential lightning flashes. Many upward lightning flashes that occur during winter thunderstorms in Japan involve more than one grounded structure (Suzuki, 1992). Wang et al. (2008) more specifically suggested that once an upward lightning discharge occurred from a high-ground object, the upward lightning triggers other upward lightning discharges of opposite polarity from nearby high-ground objects if favorable electrical charge structures of thunderstorms are available. This suggestion was later confirmed by Lu et al. (2009). Rison et al. (1999), Nag et al. (2010) and Wang et al. (2012) also observed many cases within clouds in which compact intracloud discharge (CID) initiates lightning discharge. However, evidence that an intracloud lightning discharge (IC) influences another IC, or a cloud-to-ground lightning discharge (CG), is far less commonly reported.

The electrical structure of a thunderstorm is generally three-layered (Kriehbiel, 1986). The first balloon sounding of the electric field in a thunderstorm indicating an inverted-polarity electrical structure took place in a storm near Dalhart, Texas (Marshall et al., 1995) in 1988. Rust and MacGorman (2002) presented analyses of electric field soundings indicating that some thunderstorms have an inverted structure in the vertical distribution of charge. Lightning discharges appear to deposit charge of opposite polarity in relatively localized volumes within the preexisting lower positive, midlevel negative, and upper positive charge regions associated with the potential wells (Coleman et al., 2003). The conclusions from Coleman et al. (2003),

*Corresponding author: WANG Yanhui, wyh2005@lzb.ac.cn

Riousset et al. (2007) suggested that the polarization charges carried by the leader trees could lower the net charge in the different charge layers of the thundercloud and could decrease the total electric field significantly below the lightning initiation threshold. Logically, the lightning discharge involving the main negative charge region inevitably consumes the charges and therefore suppresses the start of a new lightning discharge. However, it is possible that after a lightning discharge terminates, a new lightning discharge could be easily initiated by a lower electric field because of the remaining discharge channel of the first lightning.

The study reported in the present paper used a 3D lightning radiation source locating system (LLS) (Zhang et al., 2010) to provide evidence that IC influences another IC or CG. The interactions between these lightning discharges are also discussed.

2. Experiments and instruments

The data for the present study were obtained using a LLS (Zhang et al., 2010). The areas of study were east of Pohai Gulf (center station: Hengdian; 37.83°N, 118.08°E) in 2007–08 and the northeast edge of the Qinghai-Tibet Plateau (center station: Mingde; 37.01°N, 101.62°E) in 2009–11. The station spacing was generally around 10 km with respect to the center station, as shown in Fig. 1. Each station was equipped with: a LLS detector working at "very high frequency" (VHF) (Zhang et al., 2010) (bandwidth of 267–273 MHz), which was similar to a Lightning Mapping Array (LMA) (Rison et al., 1999), and in which the spatial and temporal development of lightning discharges are mapped by accurately timing the arrival of VHF radiation that the lightning emits; a broadband electric field change system (bandwidth of about 200 kHz to 10 MHz and a time constant of 100 μs); a fast electric field change (EFC) detector (bandwidth of about 100 kHz to 5 MHz and a time constant of 1 ms); a slow EFC detector (bandwidth of about 50 kHz to 2 MHz and a time constant of 6 s); and a field mill (dynamic range of the amplifier was ±10 V). In addition, a high precision GPS clock (±25 ns) was set at each station to synchronize all of the equipment. The outputs from all the systems were digitized and recorded on computers (Qie et al., 2009; Zhang et al., 2010). All stations were linked via a broadband wireless network system. Data collection at each station was controlled either by the central station, or operated freely. Seven stations were used to measure the arrival time, and a set of nonlinear equations was constituted (Zhang et al., 2010), where the equation could be gained for each station. This was:

$$t_i = t + \sqrt{(x_i - x)^2 + (y_i - y)^2 + (z_i - z)^2}/c, \quad (1)$$

where c is the speed of propagation of the light in a vacuum; t is the time the radiation emitted from the source location (x, y, z); (x_i, y_i, z_i) is the location of

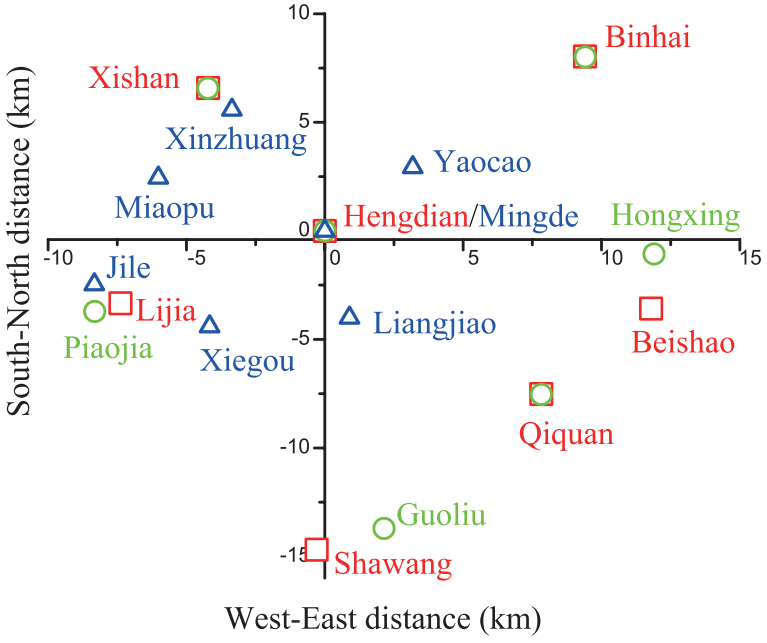

Fig. 1. Map of the measurement stations. Squares indicate the stations of the 2007 experiment; circles indicate the stations of the 2008 experiment; triangles indicate the stations of the 2010 experiment.

station i; and t_i is the arrival time at station i. The values of x, y, z, t were solved from the set of nonlinear equations, and the calculations showed that the typical horizontal error was 100 m on the network plane in the range of 100 km, the altitude error was less than 300 m, and both increased with distance.

3. Results

Usually, an IC would involve two charge regions and a CG would involve two or three charge regions (the ground was considered as a special charge region in the present study) (Rison et al., 1999; Qie et al., 2005; Rust et al., 2005; Qie, 2012). According to these features, the associated lightning discharge (including two lightning discharges at least, and following an arbitrary rule that the space-gap was less than 10 km and the time-gap was less than 800 ms between two adjacent lightning discharges) should appear as a common feature in the form of three or more charge regions being involved. This feature was found to be true, with all three pairs of associated lightning discharges involving three or more charge regions, and among them, at least one charge region was found to involve both two lightning discharges. A time-gap in time-altitude plot of the VHF-mapping image corresponding to E-field change, and a space-gap in 3D plots of the VHF-mapping image, were both employed to separate associated lightning discharges into two distinct lightning discharges. Using these two criterions, some pulses or radiation sources during time-gap could be proven to correspond to the other branch of the first lightning discharge, which was located far from the starting point of the second lightning discharges. It would be considered as two independent lightning discharges if the time-gap exceeded 60 ms or the space-gap exceeded 2 km with no apparent discharge channel connecting the two parts of the associated lightning discharge (these two values were chosen arbitrarily). These VHF-mapping radiation images did not deal with any noise filtering, and some early radiation sources could be covered by later radiation sources in the 3D plots of the VHF-mapping image (in atmospheric electricity sign convention, a negative electric field change indicates negative charge effectively transported upward). Three cases were analyzed as follows.

3.1 *Normal-polarity IC+inverted-polarity IC*

Figure 2 shows a 3D picture of a pair of associated lightning discharges in which one normal-polarity IC influenced one inverted-polarity IC at approximately 0207:48 LST 1 August 2007 (this pair of associated lightning discharges was called PAL_020748). Figure 3 shows a slow EFC and fast EFC of PAL_020748 obtained at Hengdian Station. As seen from Fig. 2, there appear to be two gaps in the altitude-time plot, lasting about 45 ms and 90 ms respectively. All radiation sources after the first time-gap were considered as secondary discharges of the first IC1 for those radiation sources distributed along the channel of IC1 seen in the 3D plots in Fig. 2. We then noted that the terminal of the part prior to the second time-gap occurred at an approximate height of 7.5 km, and the preliminary breakdown of the part after the second gap occurred at an approximate height of 6 km. Furthermore, no apparent discharge channel connecting the two parts of PAL_020748 was detected by LLS (Fig. 2), and the duration of the time-gap exceeded 60 ms. Therefore, the part of PAL_020748 after the second time-gap was considered as a separate lightning discharge.

As seen in Fig. 2, the preliminary breakdown of IC1 began at a height of approximately 7.9 km, propagating upward and reaching a height of approximately 12.0 km with a velocity of approximately 1.8×10^5 m s^{-1}. The corresponding slow EFC caused by IC1 was positive. For a vertical breakdown at height h, the reversal distance is at $d=\sqrt{2}h$, as pointed out by Shao and Krehbiel (1996). Here, the reversal distance was approximately 11.2 km, and the distance between Hengdian Station and the preliminary breakdown of IC1 was approximately 9.0 km, which was closer than the reversal distance. The polarity of the corresponding slow EFC was positive. So, the preliminary breakdown of IC1 was identified as a negative leader, and the negative charges were effectively transported upward into the upper positive charge region from the main negative charge region. In the upper positive charge region, the lightning discharges changed to develop horizontally, extending to more than 8.0 km. Furthermore, the sporadic discharge lasted approximately 90 ms in the end. In total, this normal-polarity IC lasted approximately 300 ms.

As seen in Fig. 2, the preliminary breakdown of IC2 began at a height of approximately 6.0 km, progressing downward and reaching a height of approximately 3.5 km at a velocity of approximately 2.9×10^5 m s^{-1}, forming a new connecting channel. Several intension discharge processes occurred downward along this new channel, and the corresponding slow EFC was negative. Here, the reversal distance was approximately 8.5 km, and the distance between Hengdian Station and the preliminary breakdown of IC2 was approximately 8.4 km. Considering these two values were almost equivalent, the polarity of the preliminary breakdown of IC2 was difficult to identify. The polarity of the corresponding slow EFC was negative. We noted that the channel of the initial period of IC2 developed toward Hengdian Station, as seen in the 3D plots of

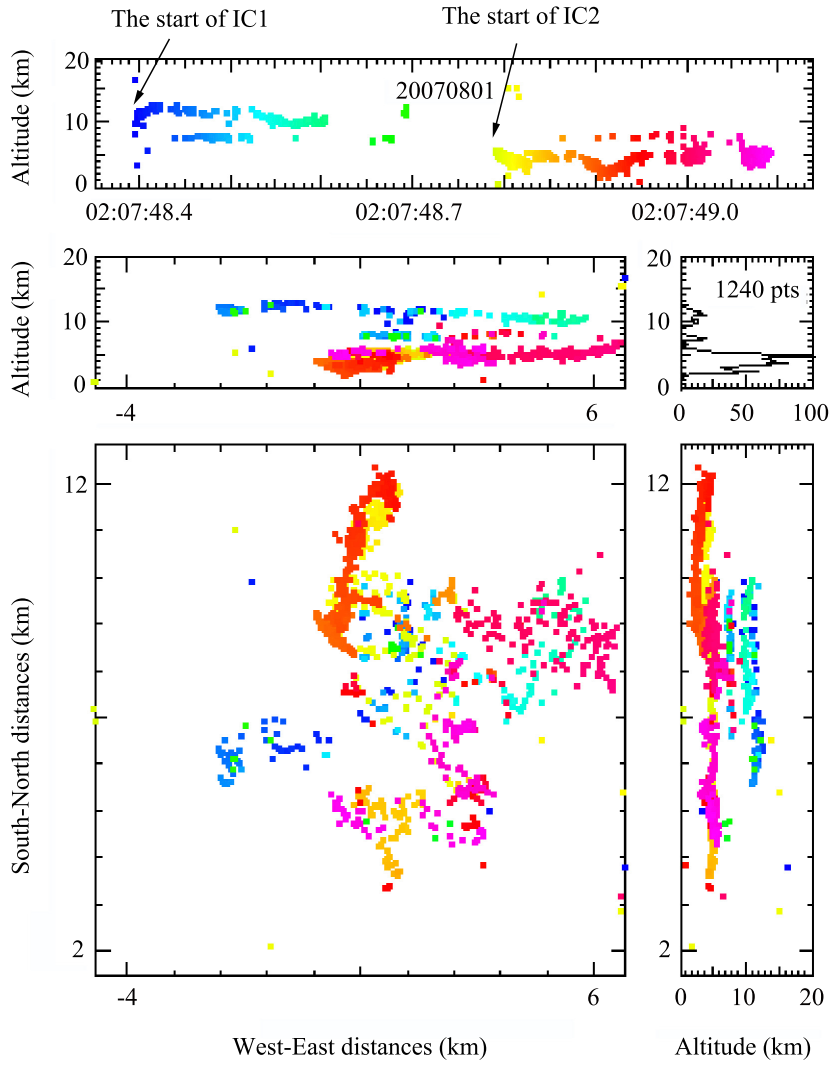

Fig. 2. VHF mapping of the associated lightning discharge PAL_020748, which included one normal-polarity IC and one inverted-polarity IC. The different colors (blue, green, yellow and red) indicate the time evolution of the VHF radiation sources. The middle-left panel shows the north–south vertical projection; the middle-right panel shows the height distribution of the number of radiation events; the bottom-left panel shows the plan view; the bottom-right panel shows the east–west vertical projections; and the origin of the coordinate is the position of the center station (Hengdian Station).

Fig. 2. So, the preliminary breakdown of IC2 was identified as a negative leader based on the definition of atmospheric electricity sign convention, and the negative charges were effectively transported downward into the lower positive charge region from the main negative charge region. Therefore, IC2 was identified as an inverted-polarity IC.

On the contrary, the positive breakdown was less well detected by the LLS in the VHF band, similar to LMA (Rison et al., 1999; Rust et al., 2005). The effect of this is that radiation events along the positive breakdown channels are usually not detected until after a time delay of typically tens of milliseconds (Rust et al., 2005). This typical phenomenon is also apparent in an inverted-polarity IC (Rust et al., 2005). It can be seen from Figs. 2 and 3 that the first and second ICs could be identified as normal-polarity and inverted-polarity ICs, respectively. As seen in Fig. 2, PAL_020748 had a three-level structure. The normal-polarity IC of PAL_020748 had a bilevel structure typ-

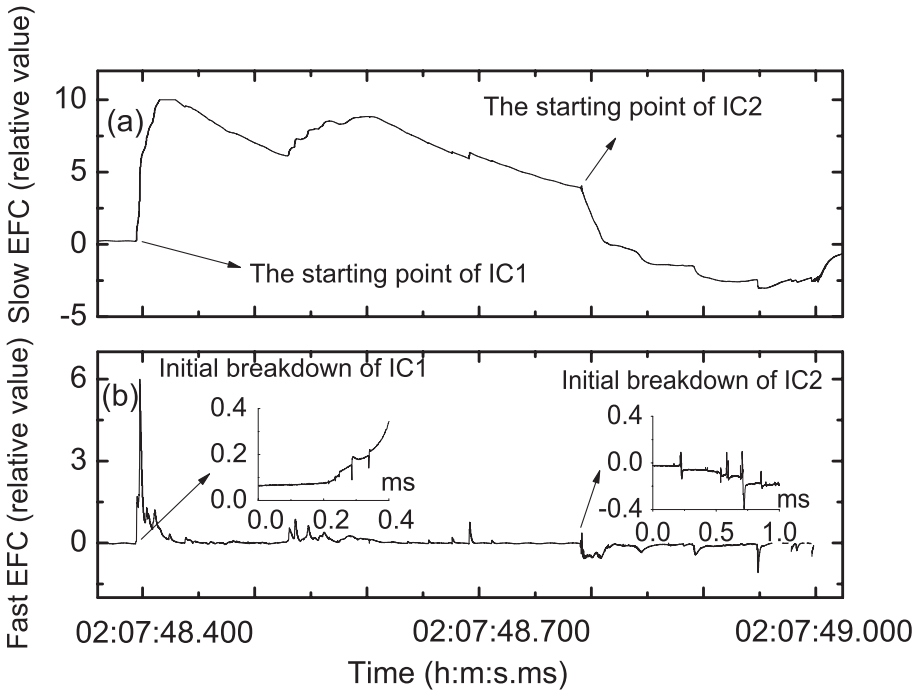

Fig. 3. The slow and fast electric field change waveforms of the PAL_020748 pair of associated lightning discharges.

ical of many ICs and similar to the results of Shao and Krehbiel (1996) and Rison et al. (1999). Furthermore, the inverted-polarity IC of PAL_020748 had an inverted bilevel structure, similar to the results of Zhang et al. (2002) and Rust et al. (2005). As seen in Fig. 2, these two opposite polarity ICs were readily distinguishable by their temporal and spatial development. Figure 2 shows that the channels of these two ICs scattered horizontally and centered at the vertical channel. The three-layer structure of the thunderstorm was roughly visible from the structure of these two ICs. The corresponding microsecond-scale fast EFCs of the preliminary breakdown of these two ICs are presented in Fig. 3b.

3.2 *Normal-polarity IC+negative CG*

Figure 4 shows a 3D picture of a pair of associated lightning discharges in which one normal-polarity IC influenced one negative CG at approximately 1339:38 LST 25 June 2008 (referred to as PAL_133938). Figure 5 shows slow and fast EFCs of PAL_133938 obtained at Xishan Station. It is regretful that the EFC waveform of the IC was absent prior to the CG. Even so, we noted that the time-gap between the first and second part of PAL_133938 exceeded 70 ms or more, as seen from both Figs. 4 and 5. Furthermore, no apparent discharge channel connecting the two parts of PAL_133938 was detected by LLS, as demonstrated in the 3D plots of Fig. 4. Therefore, PAL_133938 was considered as two independent lightning discharges, one being an IC prior to the time-gap, and the other a CG after the time-gap.

As seen in Fig. 4, the CG of PAL_133938 began at approximately 70 ms after the IC terminated. After approximately 88 ms, the step leader of this CG began, progressed downward, and then reached the ground. The discharge process then lasted approximately 200 ms after the return stroke. The preliminary breakdown of this CG started at a height of approximately 6.0 km, propagating downward and reaching a height of approximately 3.0 km. Here, the reversal distance was approximately 8.5 km. The polarity of the corresponding slow EFC was positive, and the distance between the starting point of the CG and Xishan Station was approximately 11.0 km, which was farther than the reversal distance. Therefore, the preliminary breakdown of the CG was identified as a negative leader, and negative charges in the main negative charge region were effectively transported downward into the lower positive charge region before reaching the ground. In addition, as seen in the first part of PAL_133938, the preliminary breakdown of the IC began at approximately 7 km, propagating upward and reaching a height of approximately 11 km with a velocity of approximately 1.5×10^5 m s^{-1} (a following branch of the IC began at a height of 6 km). The starting height of the IC was according to the starting height of the CG, and the horizontal distance be-

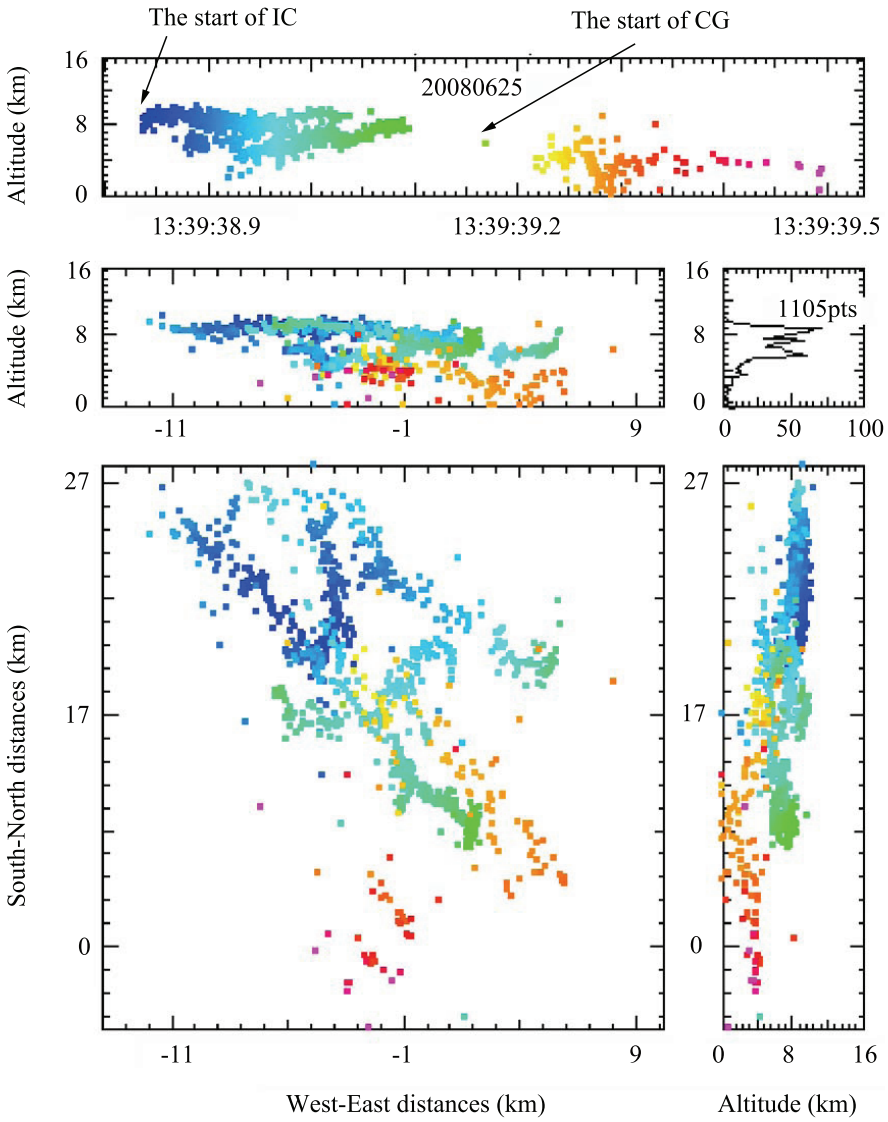

Fig. 4. VHF mapping of the PAL_133938 associated lightning discharge, which included one normal-polarity IC and one normal -CG.

tween the starting point of these two lightning discharges was less than 3 km. The preliminary breakdown of the IC was identified as a negative leader, and negative charges were effectively transported upward into the upper positive charge region. As seen in Fig. 4, the normal-polarity IC in the PAL_133938 also had a bilevel structure, similar to the normal-polarity IC in PAL_020748. This IC lasted approximately 260 ms, including two upward discharge processes. From both Figs. 4 and 5, the first and second lightning discharges of PAL_133938 were identified as a normal-polarity IC and a negative CG, respectively. The corresponding microsecond-scale fast EFCs of the preliminary breakdown of the normal-polarity IC and negative CG, and the microsecond-scale fast EFC of the return stroke of the negative CG, are presented in Fig. 5b (the microsecond-scale waveform of the return stroke was obtained at Piaojia Station).

3.3 *Inverted-polarity IC+negative CG*

Figure 6 shows a 3D picture of a pair of associated lightning discharges in which one inverted-polarity IC influenced a negative CG at approximately 1439:26 LST 7 August 2010 (referred to as PAL_143926). Figure 7 shows slow and fast EFCs of PAL_143926 obtained at Yaocao Station.

As seen from Fig. 6, the preliminary breakdown of the first part of PAL_143926 began at a height of approximately 5.5 km, progressed downward, and reached a height of approximately 3.5 km with a velocity of approximately 3.0×10^5 m s^{-1}. The first discharge channel progressed to the southwest and

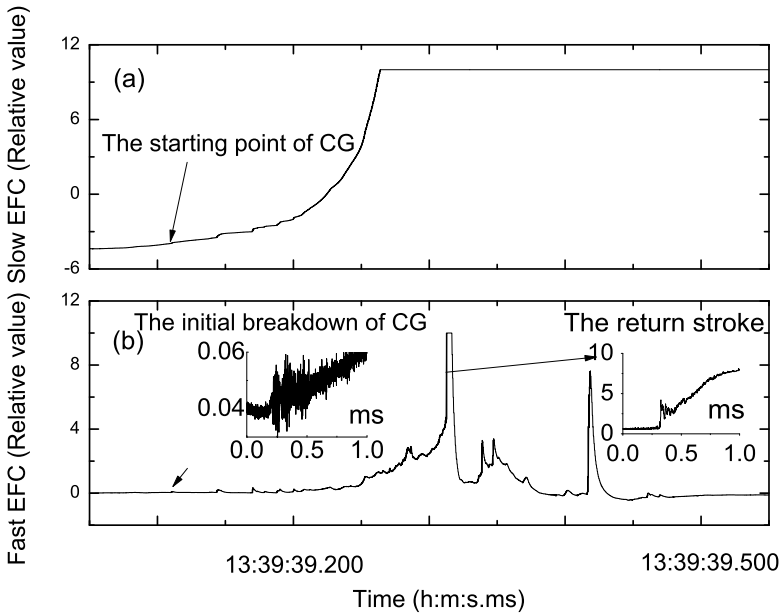

Fig. 5. The slow and fast electric field change waveforms of the PAL_133938 pair of associated lightning discharges. The microsecond-scale waveform of the return stroke came from Piaojia Station.

then turned eastward. The second discharge channel started at 3.0 km southwest of the origination point of this part, and developed back to the origination point. This part lasted approximately 100 ms. As seen in Fig. 6, the second part of PAL_143926 began at the termination of the first discharge channel of the first part, and occurred at approximately 60 ms after it terminated. In addition, the radiation sources that occurred during the 60 ms period were considered as those from another branch of the first part of PAL_143926. Furthermore, the distance between the terminal of that branch and the preliminary breakdown of the CG was more than 2.0 km. Therefore, the second part of PAL_143926 was identified as an independent CG. After approximately 50 ms, the step leader of this CG began, and then progressed downward until reaching the ground. The discharge process lasted approximately 100 ms after the return stroke.

Here, the reversal distance was approximately 7.8 km, and the distance between Yaocao Station and the starting point of the IC was approximately 10.0 km, which was farther than the reversal distance. The positive slow EFC of the IC (Fig. 7a) corresponded to the negative leader that developed downward, and the negative charges were effectively transported into the lower positive charge region. Furthermore, the preliminary breakdown of the CG began at a height of approximately 4.0 km, developing downward and reaching a height of approximately 2.5 km. Here, the reversal distance was approximately 5.7 km, and the distance between Yaocao Station and the starting point of the IC was approximately 13.5 km. Yaocao Station was outside of the reversal distance. Therefore, the positive polarity waveform of the slow EFC indicated the negative leader developed downward and negative charges were efficiently transported downward toward the ground. From both Figs. 6 and 7, the first and second ICs can be identified as an inverted-polarity IC and a negative CG, respectively. As seen in Fig. 6, and similar to the inverted-polarity IC in PAL_020748, this inverted-polarity IC also had an inverted bilevel structure. The corresponding microsecond-scale fast EFCs of the preliminary breakdown of the inverted-polarity IC and CG, and the microsecond-scale return stroke of the negative CG, are presented in Fig. 7b.

4. Discussion and conclusion

Shao and Krehbiel (1996) and Rison et al. (1999) pointed out that typical ICs usually begin between the main negative and upper positive charge regions, progress upward with time, and then move outward along the upper level channels. The radiation events along the positive breakdown channels are usually not detected until after a time delay that is typically tens of milliseconds, observed at VHF. Rakov and Uman (2003) suggested that some scenarios of lightning discharges may involve the lower positive charge

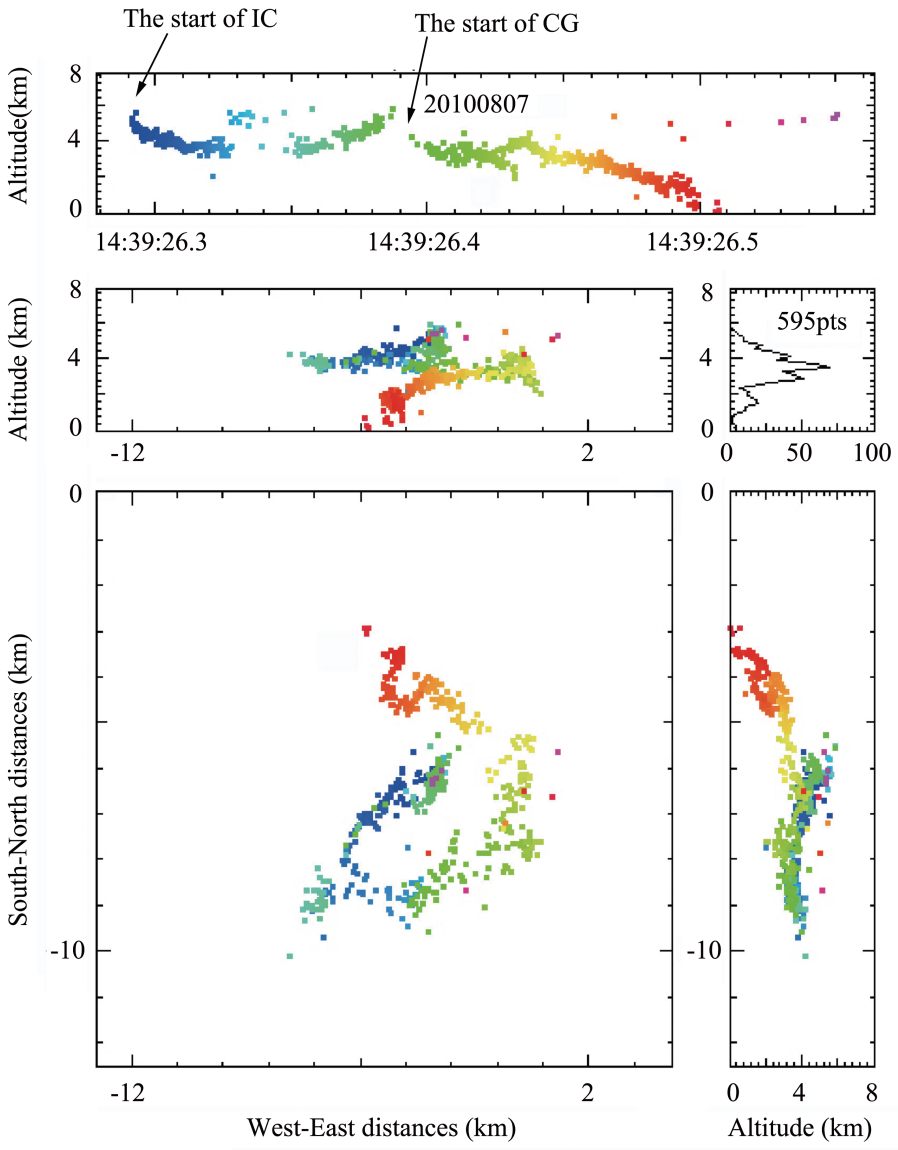

Fig. 6. VHF mapping of the PAL_143926 associated lightning discharge, which included one normal-polarity IC and one normal -CG.

region. Inverted-polarity ICs were then found in thunderstorms (Zhang et al., 2002; Rust et al., 2005) and were described as essentially 'upside-down' versions of normal-polarity ICs by Rust et al. (2005). In our study, we observed a pair of associated lightning discharges (PAL_020748) in which one normal-polarity IC influenced an inverted-polarity IC in a thunderstorm (see Fig. 2). It is worth noting (as shown by Figs. 2 and 3) that there was an opposite eventless period approximately 90 ms between the normal-polarity IC and the inverted-polarity IC. Additionally, the EFC was in a recovering stage during this period, as seen in Fig. 3a. We suggest that the electrical condition between the main negative and lower positive charge regions was insufficient to immediately initiate a new lightning discharge because numerous charges were consumed by the normal-polarity IC. During the 90 ms period, through a short-lived charge migration, the electric field recovered and gained enough energy to initiate a new lightning discharge below the main negative charge region. Furthermore, the quantity of VHF sources from an inverted IC is far more than from a normal IC, indicating that the discharge process of the inverted IC was stronger than the normal IC. In other words, the inverted IC would also occur, or would more likely occur early if no normal IC consumed negative charges in the main negative charge region. As seen in Fig. 3a, the inverted-polarity IC occurred during the recovery stage of the slow EFC caused by the normal-polarity IC. It appears that the inverted-polarity IC

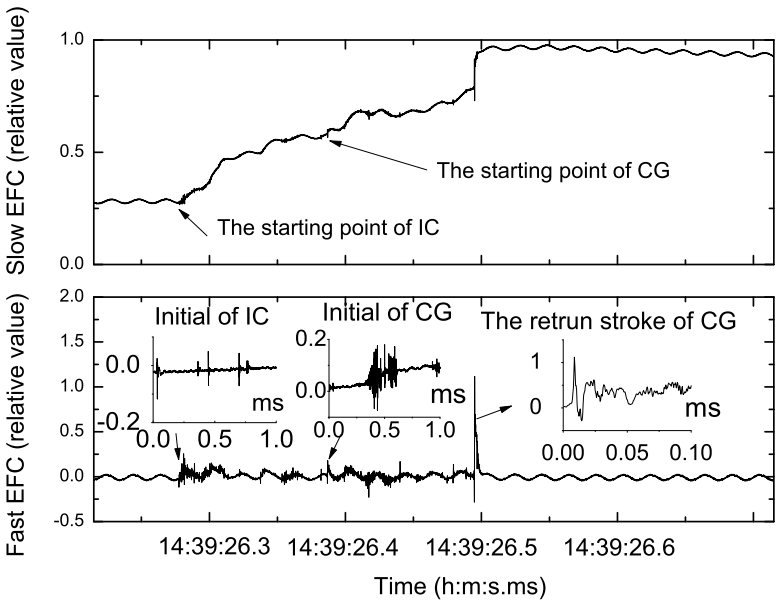

Fig. 7. The slow and fast electric field change waveforms of the PAL_143926 pair of associated lightning discharges.

might have been suppressed by the normal-polarity IC.

Rison et al. (1999) reported an example of an unusual type of CG where, instead of going directly from the main negative charge region to the ground, as usually happens, the leader to the ground was an extension of the upper level breakdown of an otherwise normal IC. Furthermore, some authors have indicated that strokes to the ground sometimes appear to be a minor branch of an extensive IC (Richard et al., 1986; Proctor et al., 1988). Fortunately, we observed two such examples, i.e. PAL_133938 and PAL_143926 (see Figs. 4 and 6). The normal-polarity IC in PAL_133938 was similar to the first case (PAL_020748) in Fig. 2, but was followed closely by a negative CG. There was also an opposite eventless period of approximately 70 ms between the normal-polarity IC and the negative CG. In addition, we noted that the distance between the main negative charge region and the land surface was closer than in PAL_020748, which we propose was one reason that the inverted-polarity IC was replaced by a negative CG, as compared with the first case (PAL_020748). Another reason may be that the charge intensity of the lower positive charge region was too low. Furthermore, the downward channel of the negative CG was interrupted, and the pulses on the fast EFC were lower, indicating the numerous charges of the main negative charge region were consumed by the normal IC, which caused the initial period of the CG discharge process to be underpowered. As seen in Fig. 5, a negative CG also occurred during the recovery stage of the slow EFC caused by the normal-polarity IC. Similar to PAL_020748, we can say that the negative CG may have been suppressed by the normal-polarity IC.

As seen in Figs. 6 and 7, the inverted-polarity IC of PAL_143926 was closely followed by a negative CG. It is worth noting that the discharge channel of the negative CG began directly at the remaining channel of the inverted-polarity IC and propagated along a new discharge channel, eventually reaching the ground. Moreover, different from the first two cases (PAL_020748 and PAL_133938), the negative CG in this case occurred during the increasing stage of the slow EFC caused by the inverted-polarity IC, as seen in Fig. 7. However, we cannot say that the subsequent lightning discharge was accelerated by the first IC because the increasing stage of the EFC could be attributed to the shielding action of the lower positive charge region being decreased by the inverted-polarity IC. In fact, the electric field between the main negative and lower positive charge regions was decreased by the first IC during this period. We noted that the first 40 ms period of the negative CG was wandering at a height range of 4–3.5 km. This indicates that the lower positive charge regions continued to consume the negative charges in the main negative charge region, preventing the initial leader from developing downward during this period. We further noted that leader was accelerated once it was through the lower positive charge region, which is in accordance with the results of Nag and Rakov

(2009). In addition, the negative CG started at the terminal of the first branch of the inverted-polarity IC, and at approximately 60 ms after it terminated, as seen in Fig. 6. It appears that the prior inverted-polarity IC provided a remaining channel to initiate the subsequent negative CG in this case.

Above all, as identified from the EFC, the subsequent lightning discharges were suppressed by the prior lightning discharges in all pairs. That is to say, the possibility of a lightning discharge below the main negative charge region was decreased by prior discharge activity. However, it is possible that the prior lightning provided a remaining discharge channel to easily initiate a new lightning discharge. The third pair of associated lightning discharges provided evidence in this regard. Even in the first two cases, we could not infer that there was no remaining discharge channel at the point where the subsequent lightning discharge occurred. In addition, whether or not the subsequent lightning, if it occurred, developed into an inverted-polarity IC or a negative CG, could be related to the distance between the main negative charge region and the land surface, as well as to the charge intensity of the lower positive charge region. One might consider, to a certain extent, that if the charges in the main negative charge region can be consumed using artificial lightning above the main negative charge regions, lightning accidents on the ground may be greatly reduced. However, it is difficult to prevent the discharge channel of the artificial lightning from developing downward and reaching the ground. Of course, the height of the main negative charge region and the charge intensity of the lower positive charge region would have to be considered carefully in any practical application of this method.

Acknowledgements. The authors are indebted to all members of the Shandong and Qinghai lightning observation experiment and the weather bureau of Shandong and Qinghai. The authors would like to thank Professors QIE Xiushu and WANG Daohong for their valuable advice. This work was supported by the National Natural Science Foundation of China (Grant Nos. 41075002, 41005022, and 40775004).

REFERENCES

Coleman, L. M., T. C. Marshall, M. Stolzenburg, T. Hamlin, P. R. Krehbiel, W. Rison, and R. J. Thomas, 2003: Effects of charge and electrostatic potential on lightning propagation. *J. Geophys. Res.*, **108**(D9), **4298**, doi: 10.1029/2002JD002718.

Kriehbiel, P. R., 1986: The electrical structure of thunderstorm. *The Earth's Electrical Environment*, E. P. Krider and R. G. Roble, Eds., National Academy Press, Washington, D.C., 90–113.

Lu, W., D. Wang, Y. Zhang, and N. Takagi, 2009: Two associated upward lightning flashes that produced opposite polarity electric field changes. *Geophys. Res. Lett.*, **36**, L05801, doi: 10.1029/2008GL036598.

Marshall, T. C., W. D. Rust, and M. Stolzenburg, 1995: Electrical structure and updraft speeds in thunderstorms over the southern Great Plains. *J. Geophys. Res.*, **100**(D1), 1001–1015, doi: 10.1029/94JD02607.

Mazur, V., 1982: Associated lightning discharges. *Geophys. Res. Lett.,* **9**(11), 1227–1230, doi: 10.1029/GL009i011p01227.

Nag, A., and V. A. Rakov, 2009: Some inferences on the role of lower positive charge region in facilitating different types of lightning. *Geophys. Res. Lett.*, **36**, L05815, doi: 10.1029/2008GL036783.

Nag, A., V. A. Rakov, D. Tsalikis, and J. A. Cramer, 2010: On phenomenology of compact intracloud lightning discharges. *J. Geophys. Res.*, **115**, D14115, doi: 10.1029/2009JD012957.

Proctor, D. E., R. Uytenbogaardt, and B. M. Meredith, 1988: VHF radio pictures of lightning flashes to ground., *J. Geophys. Res.*, **93**(D10), 12683–12727, doi: 10.1029/JD093iD10p12683.

Qie, X. S., 2012: Progresses in the atmospheric electricity researches in China during 2006–2010. *Adv. Atmos. Sci.*, **29**(5), 993–1005, doi: 10.1007/s00376-011-1195-0.

Qie, X. S., T. Zhang, C. Chen, G. Zhang, T. Zhang, and W. Wei, 2005: The lower positive charge center and its effect on lightning discharges on the Tibetan Plateau. *Geophys. Res. Lett.*, **32**, L05814, doi: 10.1029/2004GL022162.

Qie, X. S., and Coauthors, 2009: Characteristics of triggered lightning during Shandong artificial triggering lightning experiment (SHATLE). *Atmospheric Research*, **91**(2–4), 310–315.

Rakov, V. A., and M. A. Uman, 2003: Cloud Discharges. *Lightning: Physics and Effects.* Cambridge University Press, Cambridge, U. K., 321–345.

Richard, P., A. Delannoy, G. Labaune, and P. Laroche, 1986: Results of spatial and temporal characterization of the VHF-UHF radiation of lightning. *J. Geophys. Res.,* **91**(D1), 1248–1260, doi: 10.1029/JD091iD01p01248.

Riousset, J. A., V. P. Pasko, P. R. Krehbiel, R. J. Thomas, and W. Rison, 2007: Three-dimensional fractal modeling of intracloud lightning discharge in a New Mexico thunderstorm and comparison with lightning mapping observations. *J. Geophys. Res.*, **112**, D15203, doi: 10.1029/2006JD007621.

Rison, W., R. J. Thomas, P. R. Krehbiel, T. Hamlin, and J. Harlin, 1999: A GPS based three-dimensional lightning mapping system: Initial observations in central New Mexico. *Geophys. Res. Lett.*, **26**(23), 3573–3576, doi: 10.1029/1999GL010856.

Rust, W. D., and D. R. MacGorman, 2002: Possibly inverted-polarity electrical structures in thunderstorms during STEPS. *Geophys. Res. Lett.*, **29**(12),

1571, doi: 10.1029/2001GL014303.

Rust, W. D., and Coauthors, 2005: Inverted-polarity electrical structures in thunderstorms in the severe thunderstorm electrification and precipitation study (STEPS). *Atmospheric Research*, **76**(1–4), 247–271.

Shao, X. M., and P. R. Krehbiel, 1996: The spatial and temporal development of intracloud lightning. *J. Geophys. Res.*, **101**(D21), 26641–26668, doi: 10.1029/96JD01803.

Suzuki, T., 1992: Long term observation of winter lightning on Japan Sea coast. *Research Letters on Atmospheric Electricity*, **12**, 53–56.

Wang, D. H, N. Takagi, T. Watanabe, H. Sakurano, and M. Hashimoto, 2008: Observed characteristics of upward leaders that are initiated from a windmill and its lightning protection tower. *Geophys. Res. Lett.*, **35**, L02803, doi: 10.1029/2007GL032136.

Wang, Y. H, G. S. Zhang, X. S. Qie, D. H. Wang, T. Zhang, Y. X. Zhao, Y. J. Li, and T. L. Zhang, 2012: Characteristics of compact intracloud discharges observed in a severe thunderstorm in northern part of China. *Journal of Atmospheric and Solar-Terrestrial Physics.*, **84**, 7–14, doi: 10.1016/j.jastp.2012.05.003.

Zhang, G. S., Y. H. Wang, X. S. Qie, T. Zhang, Y. X. Zhao, Y. J. Li, and D. J. Cao, 2010: Using lightning locating system based on time-of-arrival technique to study three-dimensional lightning discharge processes. *Sci. China* (*D*), **53**(4), 591–602.

Zhang, Y. J., P. R. Krehbiel, and X. S. Liu, 2002: Polarity inverted intracloud discharges and electric charge structure of thunderstorm. *Chinese Science Bulletin,* **47**, 1725–1729.